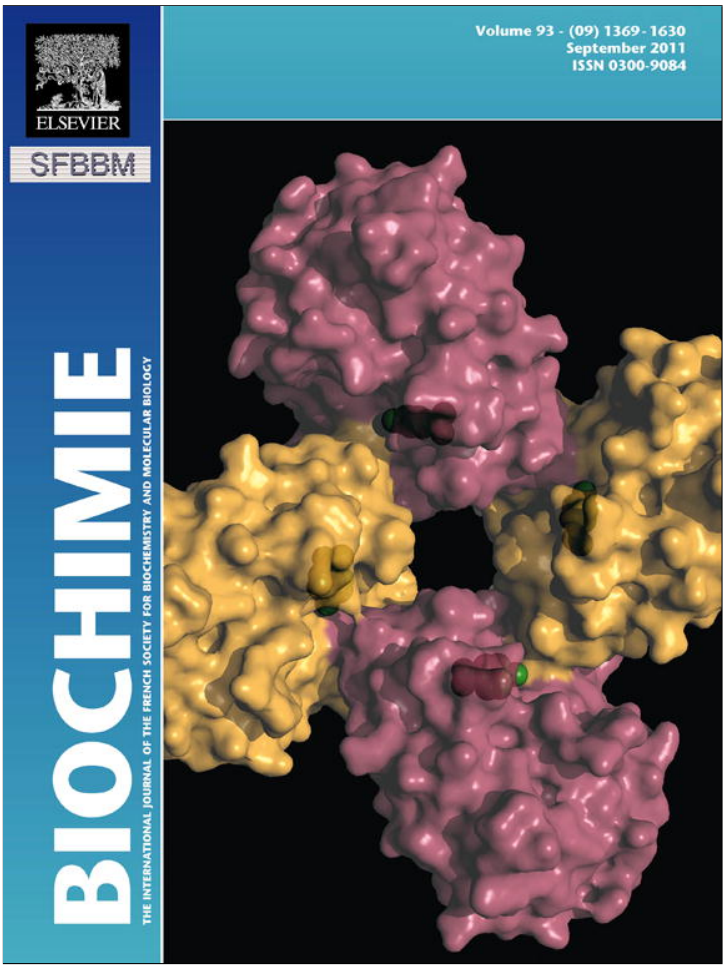

Biochimie 93 (2011) 1424–1433

Contents lists available at ScienceDirect

Biochimie

journal homepage: www.elsevier.com/locate/biochi

Research paper

Role of hydration on the functionality of a proteolytic enzyme α-chymotrypsin under crowded environment

Pramod Kumar Verma, Surajit Rakshit, Rajib Kumar Mitra**, Samir Kumar Pal*

Unit for Nano Science & Technology, Department of Chemical, Biological & Macromolecular Sciences, S.N. Bose National Centre for Basic Sciences, Block JD, Sector III, Salt Lake, Kolkata 700098, India

ARTICLE INFO

Article history:
Received 21 October 2010
Accepted 20 April 2011
Available online 29 April 2011

Keywords:
Enzyme catalysis
Water activity
Apparent specific volume
Adiabatic compressibility
Time-resolved fluorescence spectroscopy
Water relaxation dynamics

ABSTRACT

Enzymes and other bio-macromolecules are not only sensitive to physical parameters such as pH, temperature and solute composition but also to water activity. A universally instructive way to vary water activity is the addition of osmotically active but otherwise inert solvents which also mimic the condition of an intercellular milieu. In the present contribution, the role of hydration on the functionality of a proteolytic enzyme α-chymotrypsin (CHT) is investigated by modulating the water activity with the addition of polyethylene glycols (PEG with an average molecular weight of 400). The addition of PEG increases the affinity of the enzyme to its substrate, however, followed by a decrease in the turnover number (k_{cat}). Energetic calculations show that entrance path for the substrate is favoured, whereas the exit channel is restricted with increasing concentration of the crowding agent. This decrease is attributed to the thinning of the hydration shell of the enzyme due to the loss of critical water residues from the hydration surface of the enzyme as evidenced from volumetric and compressibility measurements. The overall secondary and tertiary structures of CHT determined from far-UV and near-UV circular dichroism (CD) measurements show no considerable change in the studied osmotic stress range. From kinetic and equilibrium data, we calculate 115 ± 30 numbers of water molecules to be altered during the enzymatic catalysis of CHT. Spectroscopic observation of water relaxation and rotational dynamics of ANS–CHT complex at various concentrations of the osmoting agent also support the dehydration of the hydration layer. Such dehydration/hydration processes during turnover imply a significant contribution of solvation to the energetics of the conformational changes.

1. Introduction

Almost all biological macromolecules (proteins, enzymes, and DNA) are inactive in absence of water [1–4]. The hydration shell formed by water molecules in the close vicinity of a protein plays the most significant role in protein structure, conformational changes, in substrate binding followed by enzyme catalysis, and in molecular recognition. This role of hydration in enzyme catalysis is well known and has recently been reviewed in a number of publications [1,5–7]. Dehydration makes a protein more rigid, increases its denaturation temperature and alters its physiological functionality [1,8,9]. Extensive studies show the existence of a "hydration shell" around the protein surface that excludes many solutes [10,11], and extended networks of water have been observed within protein crystal structures [12]. Hydrostatic pressure-induced changes in protein association [13] and in enzyme catalysis [14] strongly implicate changes in protein solvation through the electrostriction of water, but they remain difficult to separate from other possible density changes [15]. Hydrostatic pressure methods would not identify water that moves without density change. The induced-fit mechanism of substrate specificity [16] implies that substrate binding changes the hydration of the protein. Protein solvation has, however, been difficult to measure directly and its contribution to the energetics of conformational change is difficult to estimate.

One direct and universally applicable strategy for probing water's role is to examine the effects of reducing the availability of

Abbreviations: CHT, α-chymotrypsin; PEG, polyethylene glycol; CD, circular dichrosim; OS, osmotic stress; AMC, Ala–Ala–Phe 7-amido-4-methyl coumarin; ANS, 1-anilinonaphthalene-8-sulfonate; ES, enzyme-substrate complex; a_w, water activity; φ_v, apparent specific volume; φ_k, partial apparent adiabatic compressibility; $\Delta\nu$, Stokes shift; TRES, time-resolved emission spectra.

* Corresponding author. Present address: Noyes Laboratory of Chemical Physics, California Institute of Technology, 1200 East California Boulevard, Pasadena, CA 91125, USA.

** Corresponding author. Tel.: +91 33 2335 5705/6/7/8; fax: +91 33 2335 3477.
E-mail addresses: rajib@bose.res.in (R.K. Mitra), skpal@bose.res.in (S.K. Pal).

0300-9084/$ – see front matter © 2011 Elsevier Masson SAS. All rights reserved.
doi:10.1016/j.biochi.2011.04.017

water in protein hydration layer by the addition of osmotically active but otherwise inert solvents. Experimental and theoretical works have demonstrated large effects of osmotic stress (OS) on the thermodynamics and kinetics of many biological in vitro processes, including protein binding, folding, and aggregation [17–20]. OS has the unique feature of detecting even extremely weakly perturbed water molecules near the membrane [21] and polymer [22,23] surfaces, perturbations which sum to give large interaction energies when many such water molecules are simultaneously moved. Polyethylene glycols (PEGs) are routinely used as osmotic stressing agents to alter the water activity in solutions leading to hydration change. These polymers are highly water soluble non-charged inert macromolecules that have been used to investigate the effects of macromolecular crowding [24] as it is not expected to bind directly to the biomolecules [25]. These polymers are preferentially excluded from the hydration shells around proteins or other biomolecules. This exclusion creates an OS, which draws water away from the protein surface or out of a polymer-inaccessible crevice. Osmotically stressed enzyme environment results in a change in catalytic activity as a result of the change in the number of bound water molecules in enzyme and substrate and the enzyme-substrate complex (change in K_M, Michaelis–Menten constant) or between the ground state and transition state of the complex (change in V_{max}, maximal reaction rate). In a classic example of regulation of enzyme activity by an osmolyte [26], the dissociation constant (K_d) for glucose binding to hexokinase has been reported to decrease with increasing the osmotic pressure (OP) of the assay medium, which can be tuned by the addition of PEG in the solution [25]. A complementary approach towards the understanding of the effect of water activity (in phenomenon like dehydration) is to move away from aqueous solution completely, and study systems where even the strongly bound waters can be removed. This requires solid enzymes to be dispersed in organic solvents which lead to some remarkable properties such as greatly increased thermal stability and strikingly different substrate specificity. Low bio-catalytic activity in non-aqueous media is supposed to emanate from the poor compatibility between the solvent and enzymatic transition state [27], reduced protein flexibility [28–30], ground-state stabilization of the substrate [31], water stripping [32,33] and partial denaturation of the enzyme [30,34]. All these studies furnish evidences of the essential role of hydration and flexibility or mobility of enzyme in bio-catalytic activity. However, the exact role of hydration and flexibility of enzyme in substrate–enzyme interactions in osmotically stressed condition are still poorly understood and a detailed understanding in this field is highly demanding due to the highly compact packing in vivo condition leading to a molecular crowding [35].

This drives us in the present study in which we systemically study the role of water molecules on the substrate binding, functionality and hydration of a very commonly studied enzyme α-chymotrypsin (CHT) by modulating the solution water activity by the addition of PEG 400 (average molecular weight of 400). CHT is a proteolytic enzyme associated with the hydrolysis of peptide bonds in the mammalian digestive system. The structure of CHT [36,37], the specificity of substrates [38], the mechanism of hydrolysis, and temperature effects on catalysis and binding [39] are well-documented in the literature. In the present study the enzymatic activity of CHT on the substrate AMC (Ala–Ala–Phe 7-amido-4-methyl coumarin) is found to decrease with increasing PEG concentrations in the solution. Such a change in the activity of the enzyme with the addition of the crowding agent offers a unique opportunity to correlating its functionality with dynamics of the associated hydration layer, as the global structure and the binding site for recognition remain unchanged even at the highest concentration of PEG used, as confirmed by the far-and near-UV circular dichroism (CD) study. Densimetric and compressibility measurements of the protein in the presence of PEG provide information on the hydration state of the protein. To follow the environmental change at a particular site of the CHT upon addition of PEG, we study the fluorescence behaviour of proflavin. The overall environmental change around CHT as a function of the concentration of PEG is followed from the steady-state and time-resolved fluorescence spectroscopy of ANS (1-anilinonaphthalene-8-sulfonate), which binds rigidly at a single site on the surface of the enzyme near the Cys-1-122 disulfide bond. We also investigated the dynamical evolution at the active site of CHT as well as the hydration shell surrounding the enzyme using picosecond-resolved fluorescence anisotropy of a substrate mimic (inhibitor) proflavin and ANS.

2. Material and methods

2.1. Materials and sample preparation

Lyophilized α-chymotrypsin (CHT) powder was purchased from Sigma. ANS (1-anilinonaphthalene-8-sulfonate) and Ala-Ala-Phe 7-amido-4-methyl coumarin (AMC) were obtained from Sigma Aldrich. PEG 400 (Poly(ethylene glycol), average molecular weight of 400) was purchased from Sigma. The chemicals and the protein were used as received. All aqueous solutions were prepared in a phosphate buffer (10 mM). The PEG concentration was varied from 5% to 30% in terms of weight i.e., g PEG/(g PEG + g water).

2.2. UV–visible absorption spectroscopy

Concentration of the enzyme in the buffer was determined using the extinction coefficient (ε) value of 51 $mM^{-1}\,cm^{-1}$ at 280 nm [40]. Activity measurements were performed using AMC as the substrate. Concentration of the substrate in aqueous solution was estimated by taking the extinction coefficient value to be 15.9 $mM^{-1}\,cm^{-1}$ at 325 nm [40]. The enzyme cleaves the substrate and produces a free coumarin derivative. The absorbance of this product (coumarin derivative) was monitored in a Shimadzu Model UV-2450 spectrophotometer. The increase in the absorption at 370 nm due to the release of 7-amido-4-methyl-coumarin ($\varepsilon_{370} = 7.9\ mM^{-1}\,cm^{-1}$) was followed as a function of time. It is to be noted here that the substrate does not absorb at this monitoring wavelength. Initial rates of catalysis reactions were measured in the regime where the absorbance varies linearly with time. The reaction follows Michaelis–Menten kinetics [41] and the apparent K_M and k_{cat} values were derived by least squares fitting of the double reciprocal Lineweaver–Burk plot (Fig. 1 A). Steady-state absorption spectra were measured with a Shimadzu UV-2450 spectrophotometer.

2.3. Circular dichroism spectroscopy

Far-and near-UV circular dichroism (CD) measurements were performed on a JASCO 815 spectrometer at room temperature. Far-UV CD spectra were measured between 190 and 260 nm wavelength in 0.1 cm path length cell. Near-UV CD measurements were done in the region of 250–350 nm in 1.0 cm path length cell.

2.4. Steady-state and time-resolved fluorescence spectroscopy

Steady-state emission spectra were measured with a Jobin Yvon Fluoromax-3 fluorimeter. Fluorescence transients were measured using commercially available spectrophotometer (LifeSpec-ps) from Edinburgh Instrument, U.K. (excitation wavelength 409 nm and 375 nm, 80 ps instrument response function (IRF)) and fitted

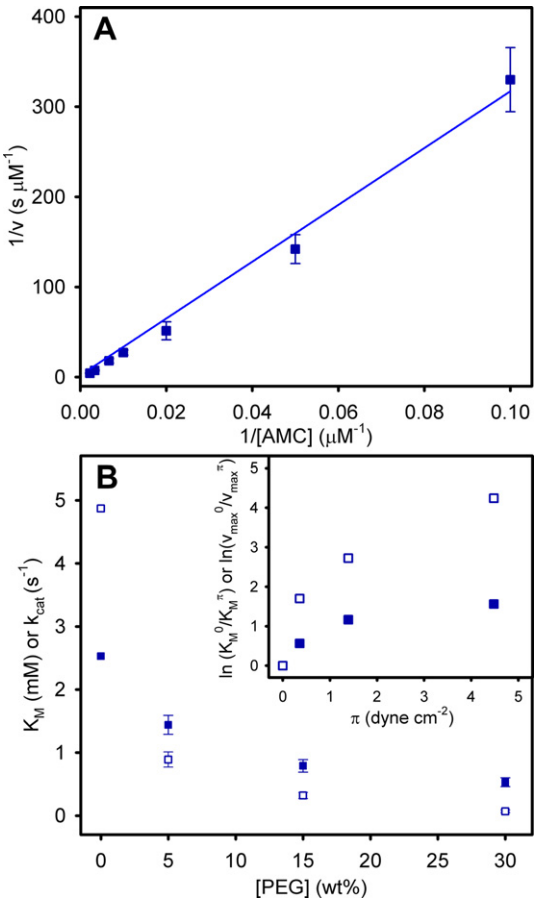

Fig. 1. A representative Lineweaver–Burk plot for the catalytic activity of CHT on the substrate AMC in presence of 5 wt% PEG (A). K_M (filled squares) and k_{cat} (open squares) for the catalytic activity of CHT on the substrate AMC as a function of PEG concentrations (B). The plot of $\ln(K_M^0/K_M^\pi)$ (filled squares) and $\ln(V_{max}^o/V_{max}^\pi)$ (open squares) against $\Delta\pi$ are shown in the inset.

using F900 software provided by Edinburgh Instrument. The details of time-resolved measurements could be found elsewhere [42]. The time dependent fluorescence Stokes shifts, as estimated from TRES (Time Resolved Emission Spectroscopy), were used to construct the normalized spectral shift correlation function or the solvent correlation function, $C(t)$ defined as

$$C(t) = \frac{\tilde{\nu}(t) - \tilde{\nu}(\infty)}{\tilde{\nu}(0) - \tilde{\nu}(\infty)} \quad (1)$$

where $\tilde{\nu}(0)$, $\tilde{\nu}(t)$ and $\tilde{\nu}(\infty)$ are the emission maxima (in cm^{-1}) at time zero, t and infinity, respectively. The $C(t)$ function represents the temporal response of the solvent relaxation process, as occurs around the probe following its photoexcitation and the associated change in the dipole moment. For anisotropy, $r(t)$ measurements emission polarization is adjusted to be parallel or perpendicular to that of the excitation, and anisotropy is defined as

$$r(t) = \frac{[I_\perp(t) - GI_{II}(t)]}{[I_\perp(t) + 2GI_{II}(t)]} \quad (2)$$

G, the grating factor, was determined following long time tail matching technique [43].

2.5. Volumetric and ultrasound velocity measurements

Volume and compressibility of CHT solution in absence and presence of PEG were calculated using the density and sound velocity values measured by a density meter (model DSA5000) from Anton Parr (Austria) with an accuracy of 5×10^{-6} g cc^{-1} and 0.5 ms^{-1} in density and sound velocity measurements, respectively. Adiabatic compressibility (β_p) of the protein solution can be determined by measuring the protein solution density (ρ_p) and the sound velocity (u_p) and applying Laplace's equation,

$$\beta_p = \frac{1}{\rho_p u_p^2} \quad (3)$$

The apparent specific volume of protein φ_v is given by

$$\varphi_v = \frac{1}{\rho_0} + \frac{\rho_0 - \rho_p}{c_p \rho_0} \quad (4)$$

where c_p is the concentration of the protein solution and ρ_0 and ρ_p are the densities of the solvent and protein solutions, respectively. The partial apparent adiabatic compressibility (φ_k) of the protein is obtained from the following relation [44,45]:

$$\varphi_k = \beta_0 \left(2\varphi_v - 2[u] - \frac{1}{\rho_0}\right) \quad (5)$$

where $[u]$ is the relative specific sound velocity increment given by

$$[u] = \frac{u_p - u_0}{u_0 c_p} \quad (6)$$

with u_0 and u_p being the sound velocities in solvent and protein solutions, respectively.

3. Results and discussion

3.1. Kinetic and structural studies

The kinetics of hydrolysis of the substrate peptide Ala–Ala–Phe-7-amido-4-methylcoumarin (AMC) by CHT has been measured sphectrophotometrically and it is found that the rate of formation of the product decreases gradually as the concentration of PEG increases in the solution. To calculate the rate constant and the turnover number, we measure the kinetics at different substrate concentrations. Fig. 1A depicts the corresponding Lineweaver–Burk plot for 5 wt% PEG concentration, where the reciprocal of the reaction velocity (v) is plotted as a function of the reciprocal of the initial concentration of AMC. A similar plot for higher concentrations of PEG is provided in the supporting information. The curves produce good linear fits for all the systems and from the slope and intercept of the curves, we calculate the Michaelis–Menten constant (K_M) and the turnover number (k_{cat}) for all the systems. The linearity of the Lineweaver–Burk plot for all the studied PEG concentrations accounts for the enzyme to follow a Michaelis–Menten mechanism even in the presence of high PEG concentration. The calculated K_M, and k_{cat} values for the three different PEG concentrations are presented in Table 1 and Fig. 1B. It is evident from the table and figure that increase in PEG concentration decreases both K_M and k_{cat} for the substrate AMC in CHT. Earlier studies by Rand et al. [25,46] reported a similar trend in which both the dissociation constant (K_d) and K_M for glucose binding of hexokinase has been found to decrease with increasing concentration of PEG. There can be two apparently acceptable mechanisms responsible for this decreased enzymatic activity, either a direct interaction of PEG with the protein active site or an osmotic stress (OS) generated by PEG that slows down the kinetics. In order to reveal whether the changes in catalytic activity induced by PEG are accompanied by alterations in the secondary and tertiary structures of α-chymotrypsin, CD measurements were performed in the far-UV (190–260 nm) and near-UV (250–350 nm) spectral ranges. As observed from Fig. 2 the aqueous CHT solution displays CD features

Table 1
Kinetics and energetics of CHT catalyzed hydrolysis of AMC at various concentrations of PEG.

[PEG] (wt%)	$\pi^{a} \times 10^{7}$ (dynes cm^{-2})	K_M (mM)	k_{cat} (s^{-1})	ΔG_M (kcal mol^{-1})	$\Delta G^{\neq}$ (kcal mol^{-1})	$\Delta G_T^{\neq}$ (kcal mol^{-1})	$\varphi_v \times 10^{-4}$ (m^3 kg^{-1})	$\varphi_k \times 10^{-14}$ (m^3 kg^{-1} Pa^{-1})
0	0	2.53[b]	4.87[c]	−3.5	16.5	13.0	7.24	2.43
5	0.357	1.44	0.89	−3.9	17.5	13.6	7.31	3.45
15	1.390	0.79	0.32	−4.2	18.1	13.9	7.46	5.23
30	4.480	0.53	0.07	−4.5	19.1	14.6	7.64	8.28

[a] From reference [22].
[b] From reference [25].
[c] From reference [25].

with minima at 202 and 232 nm (far UV-CD) and 303 nm (near UV-CD), corroborating the native secondary and tertiary structures previously reported for the enzyme [47,48]. Upon increase in the PEG concentration to 30 wt%, no significant change in the CD spectrum is observed, indicating that both the secondary and tertiary structure of the enzyme is preserved upto this PEG concentration. The CD study thus rules out any modification of the secondary or tertiary structure of the protein. At this point we can thus infer that the observed change in K_M or k_{cat} of CHT is not directly correlated to the structural modification of the active site of the enzyme, rather it is perhaps enrooted in the modification of water activity as created by the osmolyte. Covalent modification of CHT by PEG has also been reported not to perturb its tertiary structure much [49,50]. It is to be noted here that absorbance of PEG around ~200 nm and below contributes to the noise in the far UV-CD signal and we do not report the signal in this region.

3.2. Osmometric measurements

Having established the structural integrity of CHT in the presence of PEG, we now explore the idea of OS as applied by PEG on the enzymatic activity of CHT. Let us first determine the free energy changes associated with the enzymatic activity in the absence and in the presence of PEG. The trends reported here for the effect of PEG on K_M and k_{cat} can be understood by relating the changes on the free energy profile, as depicted in Scheme 1. Consider the simplest case of enzyme catalysis involving just one substrate and one enzyme-substrate (ES) complex. As observed from the linearity of the Lineweaver–Burk plot, the reaction kinetics are assumed to follow a simple Michaelis–Menten mechanism at all the studied PEG concentrations. The corresponding mechanism can be written as [51],

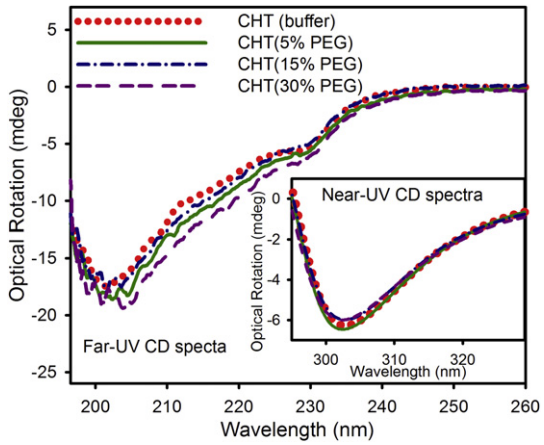

Fig. 2. The far UV-CD (circular dichroism) spectra of CHT at various wt% PEG. The near-UV-CD spectra of CHT at different wt% PEG is shown in the inset.

$$E + S \underset{k_{-1}}{\overset{k_1}{\rightleftarrows}} ES \overset{k_{cat}}{\rightarrow} \text{products} \tag{7}$$

where ES is the enzyme–substrate complex. The dissociation constant of ES, K_d ($=k_{-1}/k_1$) can be assumed to be equal to K_M for high values of k_{-1}. The corresponding free energy (ΔG_M) is generally negative valued (Scheme 1) ensuring the process to be energetically favourable. The intermediate complex then reaches a transition state ($ES^{\neq}$) with an expense of an activation free energy of $\Delta G^{\neq}$, which essentially has positive values (Scheme 1). Assuming a simplistic scheme in which E and S combine to form an activated complex $ES^{\neq}$, this then results into the product,

$$E + S \rightleftarrows ES^{\neq} \rightarrow \text{products} \tag{8}$$

the free energy associated with the formation of $ES^{\neq}$ is given by $\Delta G_T^{\neq}$ which also essentially has positive values (Scheme 1). ΔG_M can be calculated using the relation,

$$\Delta G_M = -RT \ln(1/K_d) \approx RT \ln K_M \tag{9}$$

ΔG_M can be referred to as the "entrance channel" of the substrate in which the ES complex is formed. In a similar manner formation of $ES^{\neq}$ signifies an "exit channel" in which the activated complex is cleaved to form the product and the corresponding free energy $\Delta G^{\neq}$ is related to k_{cat} and according to the activated complex theory, one can have,

$$\Delta G^{\neq} = -RT \ln\left(\frac{h}{k_B T} k_{cat}\right) \tag{10}$$

where k_B is the Boltzmann constant and h is the Plank's constant. As per Scheme 1, $\Delta G_T^{\neq}$ can algebraically be estimated as,

$$\Delta G_T^{\neq} = -RT \ln\left(\frac{h}{k_B T} \frac{k_{cat}}{K_M}\right) \tag{11}$$

The calculated ΔG_M, $\Delta G^{\neq}$ and $\Delta G_T^{\neq}$ values for all the systems are presented in Table 1. As can be observed from the table, ΔG_M value

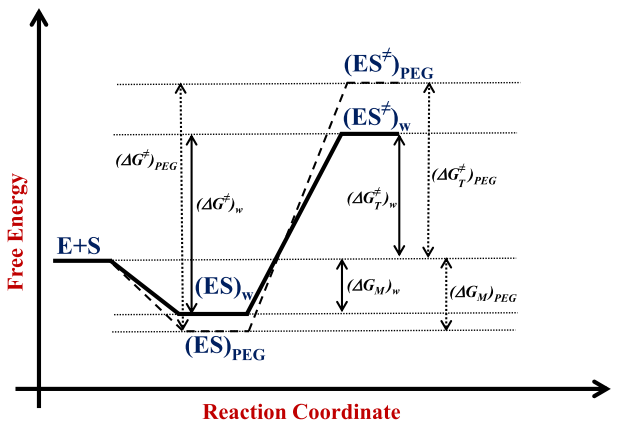

Scheme 1. Free energy changes for the simplest Michaelis–Menten kinetic scheme.

becomes more negative as PEG concentration is increased in the solution whereas, both $\Delta G^{\neq}$ and $\Delta G_T^{\neq}$ becomes more positive, indicating that the addition of PEG facilitates the formation of the *ES* complex (entrance channel) while restricts the exit channel, i.e., formation of the product. The stabilization of *ES* in the presence of PEG is more than compensated by the stabilization of $ES^{\neq}$ resulting in a higher $(\Delta G_T^{\neq})_{PEG}$ value compared to $(\Delta G_T^{\neq})_w$ (Scheme 1, Table 1) which eventually retards the enzymatic activity of CHT.

The enhancement in the affinity of CHT for AMC (decrease in ΔG_M) can be understood as follows. Addition of PEG changes the equilibrium between different conformational states of CHT by selective exclusion of PEG molecules from crevices in proteins as well as from sites at which substrates bind the enzyme. A consequence of the exclusion of PEG from certain compartments is the creation of an osmotic gradient which results in dehydration of the region inaccessible to PEG [52]. Thus, the application of osmotic pressure results in shifting the equilibrium towards the less hydrated state as has also been observed from spectroscopic as well as compressibility studies (see later). This less hydrated state makes the substrate entrance in the active site less hindered increasing the binding constant. Another equivalently possible mechanism is, in water-poor environment, the substrate does not saturate all of its hydrogen bonding propensity. Consequently, its association with CHT protein with the formation of complementary substrate-protein hydrogen bonds should be favoured by the favourable energy of hydrogen bonding resulting in further stabilization of the ES complex (Scheme 1). This is also consistent with the fact that macromolecular association constants under crowded condition increase as much as 2–3 orders of magnitude relative to those in the dilute solution [17]. Recently Griebenow et al. has reported a reduction in the substrate affinity by PEG-conjugated CHT due to steric crowding by the presence of PEG molecules near the substrate binding site [53]. Our present observation is in contrary of this finding and it clearly suggest that for the present study the active site of CHT is not modified in the presence of PEG. On the contrary, the free energy of the exit channel is increased by 2.5 kcal mol^{-1} as water is replaced with 30 wt% PEG (Table 1). Catalysis requires a critical water residue to be present in correct location and orientation such that it can initiate a nucleophilic attack followed by a loss of an H^+ ion to a nitrogen atom on His-57. The reduced water activity and partial dehydration of CHT by PEG stiffen the mobility or flexibility of the enzyme (see spectroscopic studies) and disfavour the nucleophilic attack. Furthermore, dielectric property at the enzyme's active site is decreased by PEG as evident from the spectroscopic study of proflavin-CHT complex which in turn destabilizes the polar transition state (Scheme 1). This probably perturbs the active site dynamics increasing the exit channel barrier which in turn reduces the overall catalytic efficiency of CHT. CHT in the non-aqueous environment has been reported to exhibit decreased bio-activity due to stripping of the essential water molecules from the enzymes and its rigid structure in organic solvents [54]. Both PEGylation and glycosylation of CHT increase its stability, however, its activity is decreased compared to that of the native state and this phenomenon is attributed to the restricted dynamics of the enzyme after covalent modification [49,53]. Extensively PEG-modified-CHT degrades low molecular weight substrate at rates comparable to or greater than the rates exhibited by the native enzyme but enzymatic reactions are slower for protein substrates [55]. These studies suggest our observation of modification of K_M and k_{cat} by PEG as governed mostly by the water activity modulation, rather than active site structural modification.

3.3. Change in water release under crowded condition

The exclusion of PEG from the hydration layer of CHT results in a decreased water activity (a_w) outside that compartment and subsequently removal of water from it. If ΔV_w is the change in the volume of water during the CHT-AMC binding, then at equilibrium one can write [46,56,57],

$$RT \ln a_w = \pi \Delta V_w \tag{12}$$

The free energy change during ES formation at equilibrium can be written as,

$$\Delta G_{eq}^0 = -RT \ln K_d + RT \ln a_w \tag{13}$$

Replacing a_w from equation (12) and considering ΔG_{eq}^0 to be a constant, equation (13) reduces to,

$$RT \mathrm{d} \ln K_d = \Delta V_w \mathrm{d}\pi \tag{14}$$

and assuming $K_d \approx K_M$, equation (14) transforms into,

$$\Delta V_w = \frac{RT}{\Delta \pi} \ln \left(\frac{K_M^0}{K_M^\pi} \right) \tag{15}$$

where, K_M^0 and K_M^π correspond to K_M value at the osmotic pressure (OP) of 0 and π respectively. A similar equation can be arrived from the kinetic data also in which K_M can be replaced by V_{max}. From the slope of the plot of $\ln(K_M^0/K_M^\pi)$ (or, $\ln(V_{max}^o/V_{max}^\pi)$) against $\Delta\pi$, one can calculate ΔV_w.

We plot both $\ln(K_M^0/K_M^\pi)$ and $\ln(V_{max}^o/V_{max}^\pi)$ against $\Delta\pi$ from the data obtained in Table 1 and is presented in Fig. 1B (inset). Following equation (15), the initial linear fits of the curve yield $\Delta V_w = 3825 \pm 730$ Å^3 from the kinetic data and $\Delta V_w = 3200 \pm 830$ Å^3 from the equilibrium data. The comparable values of ΔV_w obtained from the equilibrium and kinetic data signifies that the CHT-AMC binding step is the most affected step by the OS as also evident from the free energy values in which ΔG_M suffers ~30% change when water is replaced by 30% PEG, whereas the change is ~12% in the corresponding $\Delta G_T^{\neq}$ values. This observation is similar to that obtained by Rand et al. [46] in which the glucose binding step of hexokinase had been found to be mostly affected by PEG. The pooled equilibrium and kinetic data yield a change in volume of 3450 ± 860 Å^3 which is equivalent to 115 ± 30 water molecules. The numerical value of ΔN_w obtained in the present study is in good agreement with some earlier findings which report that 65–83 water molecules are associated with the binding of oxygen to haemoglobin [58,59]; binding of glucose to hexokinase results in a removal of 65 water molecules [46]; going from closed to successive open states, the ionic channels of alamethicin takes up 100 waters [60]; biting down on specific DNA complex of the restriction nuclease EcoRI sequesters 100 more water molecules than the specific complex [61]. It should be noted here that in real physiological condition this number might differ as the slopes were calculated from the initial linearity at low OP region. The curves in Fig. 1B (inset) appear steeper near the origin, a phenomenon similar to earlier reports [25,46]. It can be argued here that OS alone would dehydrate CHT to some extent so that at higher PEG concentration, less water is removed during the enzymatic process [57]. It can also be noted that at high PEG concentration the linearity is lost as PEG is expected to exchange with preferentially included water molecules at the exposed protein surface [56,62,63] making ΔN_w to be a complex function of PEG activity at the protein surface. Thus a good estimate of ΔN_w could only be drawn in the low concentration region of PEG.

3.4. Volume and compressibility measurements

The apparent specific volume (φ_v) and apparent compressibility (φ_k) of a protein are macroscopic observations which are particularly sensitive to the hydration properties of solvent exposed

atomic groups, as well as to the structure, dynamics and conformational properties of the solvent inaccessible protein interior [64–67]. In order to understand the nature of hydration of CHT under an OS, we calculate the φ_v and φ_k at different PEG concentrations and the results are presented in Table 1. In the buffer solution, the observed φ_v and φ_k values are in excellent agreement with those reported earlier for CHT in its native state [67]. As the concentration of PEG increases both φ_v and φ_k increases steadily, which can be interpreted as a reflection of a decrease in the hydration of the protein in an osmotically stressed state [68]. The change in φ_v can be rationalized accordingly; φ_v of a solute can be considered to be a cumulative contribution as given by the following equation,

$$\varphi_v = (\varphi_v)_M + (\varphi_v)_T + (\varphi_v)_I \quad (16)$$

where $(\varphi_v)_M$ is the intrinsic specific volume of the protein, which corresponds to the domain which water cannot penetrate, $(\varphi_v)_T$ is the "thermal volume" which corresponds to the free volume including voids or cavities formed by the folding of polypeptide chain. $(\varphi_v)_I$ refers to as the "interaction volume" which is related to the change in the solvent volume due to hydration. Assuming $(\varphi_v)_M$ to remain unaffected by OS, the change in φ_k can be given as,

$$\Delta\varphi_v = \Delta(\varphi_v)_T + \Delta(\varphi_v)_I \quad (17)$$

which can be equated to [67],

$$\Delta\varphi_v = \Delta(\varphi_v)_T + \Delta n_h\left(\frac{\overline{V_h} - \overline{V_0}}{M}\right) \quad (18)$$

where $\overline{V_h}$ and $\overline{V_0}$ are the partial molar volumes of water in the hydration shell and in the bulk state respectively, M is the molecular weight of the protein, Δn_h is the change in the number of hydration shell water molecules. Earlier studies suggest that $(\varphi_v)_I$ is the only component of the φ_v of a protein that is sensitive to hydration. Thus $\Delta\varphi_v$ can be assumed to be largely contributed by the change in the interaction volume only. It can be noted here that $(\varphi_v)_I$ contributes a negative share towards φ_v due to the smaller value of $\overline{V_h}$ compared to $\overline{V_0}$ [69]. The positive $\Delta\varphi_v$ obtained in the present study (Table 1) thus has contribution from the negative value of Δn_h which indicates a dehydration of the protein hydration layer upon addition of PEG. A rough estimate of the extent of hydration could be made by assuming $\Delta\varphi_v$ to be solely contributed by $(\varphi_v)_I$, and rewriting equation (18) as,

$$\Delta\varphi_v \approx \Delta n_h\left(\frac{\overline{V_h} - \overline{V_0}}{M}\right) \quad (19)$$

Taking $\Delta\varphi_v$ to be 0.4×10^{-4} m^3 kg^{-1} for 30% PEG and assuming $\overline{V_h}$ to be $\sim$11 cm^3 mol^{-1} [69], we get $\Delta N_w \sim 150$ i.e., addition of 30% PEG dehydrates each CHT molecule by 150 water molecules. Considering the total surface area of charged and polar atomic groups of CHT to be $\sim$5230 Å^2 [67], and assuming a monolayer close packed hydration, it corresponds to $\sim$18% dehydration of the protein. It can be noted here that this value is a simplified one and does not consider the contribution from $(\varphi_v)_T$ and also does not take into account the multiple solvation layer in the protein surface. However, this decrease in hydration layer is in good agreement with the 12% decrease in $\Delta G_T^{\neq}$ for the catalytic activity (Table 1), which clearly establishes the role of OS upon dehydration followed by the retardation in the catalytic activity.

A similar agreement holds good for the compressibility measurement in which the change in $\Delta\varphi_k$ could be assumed to be arising due to the sole contribution from the hydration compressibility. The positive $\Delta\varphi_k$ (Table 1) clearly indicates an increase in the water compressibility due to the increased interaction of water molecules with the solvent exposed atomic groups of the enzyme [67,70,71]. The increased φ_k thus has its origin in exclusion of hydration layer water molecules making it thin which has also been confirmed from the spectroscopic studies (see later). These highly structured water molecules thus act as a poor nucleophile resulting in a retarted rate of enzyme kinetics at higher PEG concentrations (Table 1).

3.5. Spectroscopic measurement

After establishing the phenomenon of dehydration of CHT hydration layer under an OS generated by PEG molecules, we now investigate its site specificity using steady-state and time-resolved fluorescence spectroscopy. A chromophoric inhibitor of the enzyme (proflavin) is used as a spectroscopic probe to monitor the change in local polarity of the enzyme's active site. Local polarity is the polarity experienced by a probe molecule at the microscopic scale; it is an important parameter for monitoring the local environment such as binding sites of proteins, surfactant self-assembly systems, and reverse micelles as modest changes in local polarity lead to variation in physical as well as chemical properties. Experimental studies suggest that the dye binds the protein at a single site in the vicinity of the active centre [36,72]. Fig. 3 (inset) shows the difference absorption spectra of proflavin in CHT at different PEG concentrations, in which the absorption spectrum of proflavin in CHT adduct has been subtracted from that of the buffer. It is evident from the figure that the absorbance peak suffers a progressive shift towards higher wavelength with the increase in PEG concentration [38]. The observed red-shift indicates a strong binding of the inhibitor to the catalytic site and a subsequent decrease in the local polarity around the enzyme's active site, a phenomenon very similar to the spectral perturbation as observed when proflavin is dissolved in apolar solvents [38]. Fig. 3 depicts the emission spectrum of proflavin in CHT, and it is found that the fluorescence maximum shifts towards lower wavelength with the addition of PEG indicating a decrease in the polarity around the probe, which corroborates the absorption results. In an earlier study Krishtalik et al. [73] measured the Stokes shift of proflavin in CHT film as a function of humidity and found that the Stokes shift and reorganization energy (defined as the energetic cost of repolarization of the surrounding medium, λ_s) decreases with decreasing water content. They concluded that the decrease in λ_s, compared to the solvated proflavin-CHT complex, is apparently related to the removal of hydration shell water surrounding the protein. In the

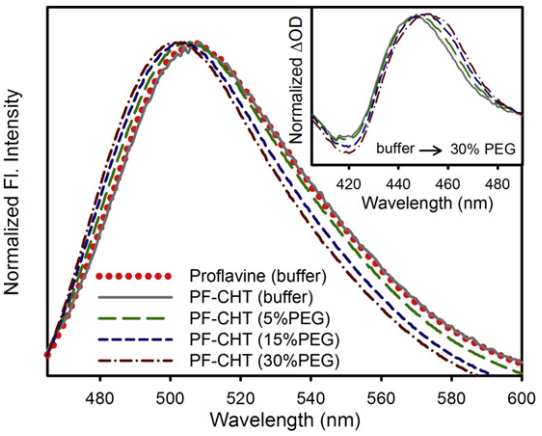

Fig. 3. Emission spectra of proflavin in buffer, and CHT with various wt% PEG (λ_{ex} = 409 nm). Difference absorption spectra of proflavin in CHT (with respect to proflavin in buffer) with 0, 5, 15 and 30 wt% PEG is shown in the inset.

present study, addition of the PEG decreases Stokes shift ($\Delta\nu$) from 2939 cm^{-1} (in buffer) to 2194 cm^{-1} (in 30% wt PEG) (Table 2) indicating a lower polarity and hence a lower dielectric property experienced around the enzyme's active site which is an outcome of stripping of some water molecules from the protein surface in the presence of PEG. This decrease in dielectric properties also destabilizes the polar transition state thereby decreasing the rate of product formation (Table 1 and Scheme 1).

3.6. Hydration dynamics under crowded condition

To specifically examine the local hydration dynamics at the surface of the enzyme CHT, the fluorescence behaviour of the probe ANS, commonly used to monitor structural changes of proteins and membranes, is studied at various PEG concentrations. Previous extensive fluorescence study [72] followed by an X-ray study [36] of the CHT–ANS complex specify that ANS binds rigidly (binding constant of the order of 10^4 M^{-1}) at a single site on the surface of the protein near the Cys-1–122 disulfide bond, a site which is almost opposite in the position to the enzymatic centre. These studies also conclude that the local environment around ANS in the complex is identical both in the solution as well as in the crystalline phase. In Fig. 4, we present the steady-state fluorescence spectra of CHT–ANS solutions in buffer and at three different PEG concentrations. It is found that the steady-state fluorescence intensity of ANS in CHT is much higher than that in the buffer and the emission maximum of ANS in CHT (~465 nm) is markedly blue shifted compared to that in buffer (~520 nm) indicating that the local polarity around ANS and hence at the enzyme's surface is lower compared to that in bulk water. Earlier studies show that the emission maximum of ANS displays a marked blue-shift with decreased solvent polarity with a consequent increase in the quantum yield [74]. The fluorescence intensity of ANS bound to CHT is found to decrease along with a small red-shift with the addition of PEG (Fig. 4), which suggests that ANS binding site is now experiencing higher polarity and hence greater contribution from bulk type water compared to that in the absence of PEG. Higher contribution from bulk type water in the presence of PEG could be due to the thinning of the hydration layer as observed form compressibility study and/or faster exchange between surface-bound to bulk type water molecules as elucidated in the following discussions. To understand the dynamic nature of water molecules at the protein surface, we study the time-resolved fluorescence spectroscopy of ANS in the presence of PEG. Fig. 5A (inset) shows the fluorescence transients of ANS-CHT adduct in the buffer at three selected wavelengths of 400, 460 and 520 nm. The transient at 460 nm can be fitted tetra-exponentially with time components of 0.03 ns (61%), 0.33 ns (17%), 1.9 ns (15%) and 7.0 ns (7%), whereas for the extreme red wavelength (520 nm), a distinct rise component of 0.18 ns is obtained along with a decay component of 14.0 ns. The presence of faster decay components at the blue end and a rise component at the red wavelength is consistent with the picture of solvation dynamics, a phenomenon which represents the rate at which the solvent dipoles/charged species are rearranged surrounding an instantaneously created dipole (a detailed description could be found in the supporting information). With the

Table 2
Steady-state absorption and emission peaks of proflavin bound to CHT (active centre) at different concentrations of the PEG.

[PEG] (wt%)	Absorbance peak (nm)	Emission peak (nm)	Stokes shift (cm^{-1})
0	443	508	2934
5	447	505	2569
15	450	504	2381
30	453	503	2194

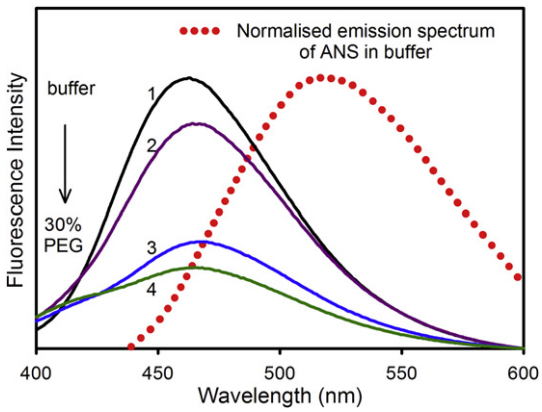

Fig. 4. Emission spectra of free ANS in buffer, and CHT with various wt% PEG ($\lambda_{ex} = 375$ nm).

increase in PEG concentrations, the transients still show wavelength dependency, however, with a decrease in the time constants (data not shown). Using the decay transients at different wavelengths, we construct the time-resolved emission spectra (TRES) for all the systems. A representative TRES for ANS-CHT in the buffer is presented in Fig. 5A which shows a significant dynamic fluorescence Stokes shift of 1256 cm^{-1} in 8 ns (Table 3). Fig. 5B shows the $C(t)$ plot of ANS-CHT in the buffer, 5 wt% and 30 wt% PEG

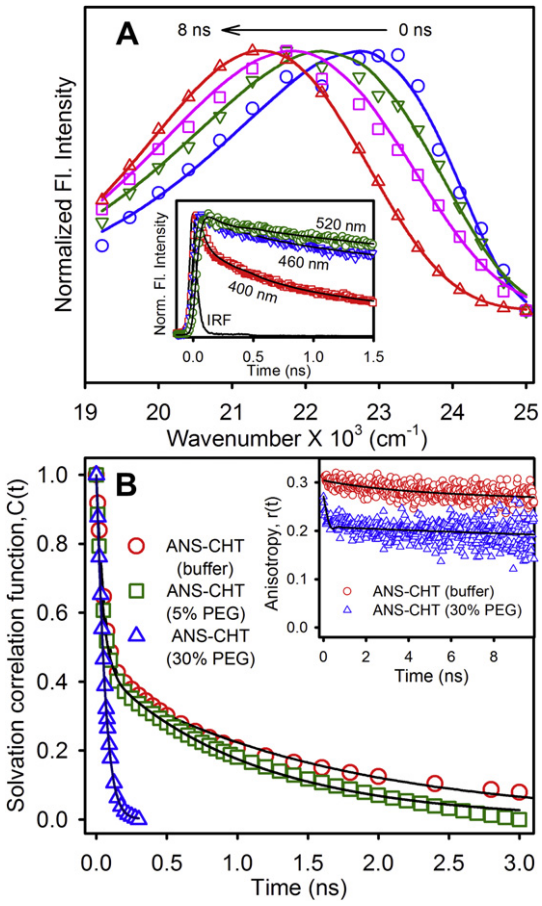

Fig. 5. Time-resolved emission spectra (TRES) for ANS-CHT complex in buffer (A). Picosecond-resolved fluorescence transients of ANS-CHT adduct in buffer is shown in the inset (A). Solvation correlation function, $C(t)$, of ANS-CHT adduct in buffer and 5 and 30 wt% PEG (B). Time-resolved anisotropy decay, $r(t)$, of ANS-CHT in buffer and 30 wt% PEG is shown in the inset (B).

Table 3
Solvation correlation time constants and rotational time constants of ANS at the enzyme (CHT) surface at various concentrations of PEG.

[PEG] (wt%)	Solvation time constants			$\Delta\nu$ (cm^{-1})	Rotational time constants	
	τ_1 (ns)	τ_2 (ns)	$<\tau>$ (ns)		τ_1 (ns)	τ_2 (ns)
0	0.06 (59%)	1.64 (41%)	0.71	1256	2.89	48
5	0.06 (55%)	1.14 (45%)	0.50	801	1.29	46
30	0.06 (100%)	–	0.06	597	0.10	40

concentrations constructed using equation (1). The $C(t)$ plots are fitted bi-exponentially and the corresponding solvation time constants are presented in Table 3. In aqueous CHT solution a fast component of 60 ps is obtained along with a slow component of 1.64 ns, which decreases to 1.07 ns at 5 wt% PEG and eventually vanishes at 30% PEG (Table 3). It should be noted here that both the observed time constants (slow and fast) are much slower than the subpicosecond solvation time constant of bulk water [75,76]. Water molecules in protein surface and in other organized assemblies exhibit ultraslow component of solvation dynamics in 100–1000 ps time scale [77,78]. Bagchi et al. proposed the presence of at least two types of water molecules at the protein surface and these water molecules remain in a dynamic equilibrium with the bulk or free type water molecules as expressed below [79,80].

$$\mathrm{Water}_{\text{surface bound}} \underset{k_{fb}}{\overset{k_{bf}}{\rightleftarrows}} \mathrm{Water}_{\text{bulk}} \tag{20}$$

where k_{bf} and k_{fb} are the rate constants related to the transition between surface-bound to bulk water molecules. This equilibrium is sensitive to the change in the microenvironment of the protein, e.g. temperature, pressure, additives etc. As has been observed in the earlier sections, addition of PEG produces an OS in the hydration layer, which in turn shifts the equilibrium towards a less hydrated conformation and also increases the contribution of faster moving bulk water molecules around the enzyme's surface. This explains the observed red-shift in the steady state emission (Fig. 4) and also decrease in the average solvation time constant $<\tau>$ ($=a_1\tau_1 + a_2\tau_2$ where τ_i represents the solvent correlation time constant and a_i represents its relative percentage.) with increasing PEG concentrations (Table 3). It should be taken into consideration that the origin of the slow component could be due to the collective contribution from both the bound type water as well as from the segmental motion of the protein residues. Sahu et al. [81] earlier reported slow solvation time component (4.5 ns) for ANS bound to BSA. They attributed this slow component due to the segmental motion of the protein residues. It should be mentioned here that in the BSA-ANS complex, ANS resides deep inside the lipid-binding cavity of the protein and hence the contribution from the protein residue is the major one, whereas in the present study, the presence of a faster component of 60 ps in the aqueous environment, signifies the location of ANS in the hydration layer of CHT. The disappearance of the slow component at high PEG concentration also suggests that ANS binding site of the enzyme is experiencing more contributions from bulk type water due to partial removal of water from hydration sheath and hindrance to the segmental motion of the protein residues which in turn decreases conformational flexibility of the enzyme. To gain further insight we analyse the lifetime of ANS bound to CHT at different PEG concentrations and found that the contribution of 14 ns lifetime component, characteristic of ANS–CHT adduct, decreases from 44% (in the buffer) to 9% (30 wt% PEG). This observation is consistent with the decrease in fluorescence intensity of ANS with the increasing concentration of PEG. Thus the faster dynamics at the higher concentration of PEG suggests thinning of the hydration water shell around the enzyme.

To further confirm the modification of the enzyme's surface with the addition of PEG, we measure the temporal anisotropy decay, $r(t)$, of the probe ANS bound to CHT in buffer and 5 wt% and 30 wt% PEG concentrations. Free ANS exhibits a fast single exponential rotational decay with time constant of 60 ps in methanol and 90 ps in buffer, respectively [82]. On the other hand the rotational relaxation of ANS bound to CHT has been found to decay bi-exponentially (Table 3, Fig. 5B inset) which has its origin in the two processes involved viz. the overall tumbling of the ANS bound enzyme (slow component) and the internal rotation of the fluorophore relative to the enzyme molecule i.e., wobbling of the probe (fast component). With the addition of PEG these components get faster indicating a greater contribution from the bulk type of water molecules as has also been observed in the solvation dynamics study. However, ANS is still bound to the surface of the enzyme even at 30 wt% PEG concentration as evident from the presence of a slow component of the rotational time constant. In a controlled study, we ensure that similar slow rotational time constants are not found in 5 wt% and 30 wt% PEG solution without the enzyme.

4. Conclusions

Our results show that the enzymatic activity of CHT decreases with the addition of an osmotic/crowding agent, PEG 400. A detailed energetic calculation showed that the entrance path for the substrate is stabilized (decrease in K_M) whereas the exit channel is destabilized (decrease in k_{cat}) with increasing osmotic stress (OS). This decrease is attributed to the loss of critical water residues from the hydration shell of the enzyme. The overall secondary and tertiary structures of CHT determined from far UV and near UV-CD show no significant change in the studied osmotic stress range, ruling out the possibility of massive structural reorientation of the overall enzyme being responsible for the altered catalytic activity. From kinetic and equilibrium data, we calculate 115 ± 30 water molecules to be altered during the enzymatic catalysis of CHT on AMC. Densimetric and compressibility measurements also support the expulsion of water molecules from the hydration layer of the enzyme under OS. This observation is also confirmed by studying spectroscopic properties of proflavin, a substrate mimic, in the active site of the CHT. The application of osmotic pressure shifts the equilibrium towards the less hydrated state for any system of equilibrium between two states of unequal hydration. We reconfirm this fact by observing the hydration and rotational dynamics of ANS-CHT complex at various concentrations of the osmoting agent. Our findings highlight the significance of the alteration of hydration under crowded environment, which is often encountered in real biological systems.

Acknowledgement

P.K.V and S.R. thank CSIR for research fellowships. We thank DST for a financial grant (SR/SO/BB-15/2007).

Appendix. Supplementary data

Supplementary data associated with this article can be found in the online version, at doi:10.1016/j.biochi.2011.04.017.

References

[1] J.A. Rupley, G. Careri, Protein hydration and function. in: F.M.R.J.T.E.C.B. Anfinsen, S.E. David (Eds.), Adv. Protein Chem. Academic Press, 1991, pp. 37–172.

[2] A. Frolich, F. Gabel, M. Jasnin, U. Lehnert, D. Oesterhelt, A.M. Stadler, M. Tehei, M. Weik, K. Wood, G. Zaccai, From shell to cell: neutron scattering studies of biological water dynamics and coupling to activity, Faraday Discuss 141 (2009) 117–130.

[3] P. Ball, Water as an active constituent in cell biology, Chem. Rev. 108 (2008) 74–108.

[4] Discussion meeting issue 'The molecular basis of life: is life possible without water?', Phil. Trans. R. Soc. Lond. B 359 (2004) 1143–1328.

[5] J.A. Kornblatt, M.J. Kornblatt, Water as it applies to the function of enzymes, Int. Rev. Cytol. 215 (2002) 49–73.

[6] Y. Pocker, Water in enzyme reaction: biophysical aspects of hydration–dehydration processes, Cell. Mol. Life Sci. 57 (2000) 1008–1017.

[7] L. Yang, J.S. Dordick, S. Garde, Hydration of enzyme in nonaqueous media is consistent with solvent dependence of its activity, Biophys. J. 87 (2004) 812–821.

[8] J. Partridge, P.R. Dennison, B.D. Moore, P.J. Halling, Activity and mobility of subtilisin in low water organic media: hydration is more important than solvent dielectric, Biochim. Biophys. Acta (BBA): Protein Struct. Mol. Enzymol. 1386 (1998) 79–89.

[9] P.J. Halling, What can we learn by studying enzymes in non–aqueous media? Philos. Trans. R. Soc. Lond. Ser. B Biol. Sci. 359 (2004) 1287–1297.

[10] T. Arakawa, S.N. Timasheff, The stabilization of proteins by osmolytes, Biophys. J. 47 (1985) 411–414.

[11] T. Arakawa, S.N. Timasheff, Mechanism of polyethylene glycol interaction with proteins, Biochemistry 24 (1985) 6756–6762.

[12] E. Meyer, Internal water molecules and H-bonding in biological macromolecules: a review of structural features with functional implications, Protein Sci. 1 (1992) 1543–1562.

[13] G. Weber, H.G. Drickamer, The effect of high pressure upon proteins and other biomolecules, Q. Rev. Biophys. 16 (1983) 89–112.

[14] P.S. Low, G.N. Somero, Activation volumes in enzymic catalysis: their sources and modification by low-molecular-weight solutes, Proc. Natl. Acad. Sci. U.S.A. 72 (1975) 3014–3018.

[15] D.A. Plager, G.L. Nelsestuen, Dissociation of peripheral protein-membrane complexes by high pressure, Protein Sci. 1 (1992) 530–539.

[16] D.E. Koshland, The Enzymes. Academic Press, New York, 1959.

[17] B. van den Berg, R.J. Ellis, C.M. Dobson, Effects of macromolecular crowding on protein folding and aggregation, EMBO J. 18 (1999) 6927–6933.

[18] B. van den Berg, R. Wain, C.M. Dobson, R.J. Ellis, Macromolecular crowding perturbs protein refolding kinetics: implications for folding inside the cell, EMBO J. 19 (2000) 3870–3875.

[19] M.S. Cheung, D. Klimov, D. Thirumalai, Molecular crowding enhances native state stability and refolding rates of globular proteins, Proc. Natl. Acad. Sci. U.S.A. 102 (2005) 4753–4758.

[20] V.N. Uversky, E.M. Cooper, K.S. Bower, J. Li, A.L. Fink, Accelerated α-synuclein fibrillation in crowded milieu, FEBS Lett. 515 (2002) 99–103.

[21] R.P. Rand, V.A. Parsegian, Hydration forces between phospholipid-bilayers, Biochim. Biophys. Acta 988 (1989) 351–376.

[22] D.C. Rau, B. Lee, V.A. Parsegian, Measurement of the repulsive force between polyelectrolyte molecules in ionic solution: hydration forces between parallel DNA double helices, Proc. Natl. Acad. Sci. U.S.A. 81 (1984) 2621–2625.

[23] D. Rau, V. Parsegian, Direct measurement of forces between linear polysaccharides xanthan and schizophyllan, Science 249 (1990) 1278–1281.

[24] R.J. Ellis, Macromolecular crowding: obvious but underappreciated, Trends Biochem. Sci. 26 (2001) 597–604.

[25] C. Reid, R.P. Rand, Probing protein hydration and conformational states in solution, Biophys. J. 72 (1997) 1022–1030.

[26] V.A. Parsegian, R.P. Rand, D.C. Rau, Macromolecules and water: probing with osmotic stress, Methods Enzymol. 259 (1995) 43–94.

[27] P.C. Michels, J.S. Dordick, D.S. Clark, Dipole formation and solvent electrostriction in subtilisin catalysis, J. Am. Chem. Soc. 119 (1997) 9331–9335.

[28] V.M. Suzawa, Y.L. Khmelnitsky, L. Giarto, J.S. Dordick, D.S. Clark, Suspended and immobilized chymotrypsin in organic media: structure–function relationships revealed by electron spin resonance spectroscopy, J. Am. Chem. Soc. 117 (1995) 8435–8440.

[29] P.A. Burke, R.G. Griffin, A.M. Klibanov, Solid-State nuclear magnetic resonance investigation of solvent dependence of tyrosyl ring motion in an enzyme, Biotechnol. Bioeng. 42 (1993) 87–94.

[30] R. Affleck, Z.F. Xu, V. Suzawa, K. Focht, D.S. Clark, J.S. Dordick, Enzymatic catalysis and dynamics in low-water environments, Proc. Natl. Acad. Sci. U.S.A. 89 (1992) 1100–1104.

[31] K. Ryu, J.S. Dordick, How do organic solvents affect peroxidase structure and function? Biochemistry 31 (1992) 2588–2598.

[32] L.A.S. Gorman, J.S. Dordick, Organic solvents strip water off enzymes, Biotechnol. Bioeng. 39 (1992) 392–397.

[33] A. Zaks, A.M. Klibanov, Enzyme-catalyzed processes in organic solvents, Proc. Natl. Acad. Sci. U.S.A. 82 (1985) 3192–3196.

[34] P.A. Burke, R.G. Griffin, A.M. Klibanov, Solid-state NMR assessment of enzyme active center structure under nonaqueous conditions, J. Biol. Chem. 267 (1992) 20057–20064.

[35] A.P. Minton, The influence of macromolecular crowding and macromolecular confinement on biochemical reactions in physiological media, J. Biol. Chem. 276 (2001) 10577–10580.

[36] L.D. Weber, A. Tulinsky, J.D. Johnson, M.A. El-Bayoumi, Expression of functionality of α-chymotrypsin. The structure of a fluorescent probe-α-chymotrypsin complex and the nature of its pH dependence, Biochemistry 18 (1979) 1297–1303.

[37] P.B. Sigler, D.M. Blow, B.W. Matthews, R. Henderson, Structure of crystalline α-chymotrypsin: II. A preliminary report including a hypothesis for the activation mechanism, J. Mol. Biol. 35 (1968) 143–164.

[38] S.A. Bernhard, B.F. Lee, Z.H. Tashjian, On the interaction of the active site of α-chymotrypsin with chromophores: proflavin binding and enzyme conformation during catalysis, J. Mol. Biol. 18 (1966) 405–420.

[39] F.C. Wedler, L.S. Uretsky, G. McClune, J. Cencula, Conformational states of chymotrypsin at high pH: temperature effects on catalysis and binding, Arch. Biochem. Biophys. 170 (1975) 476–484.

[40] R. Biswas, S.K. Pal, Caging enzyme function: α-chymotrypsin in reverse micelle, Chem. Phys. Lett. 387 (2004) 221–226.

[41] A. Fersht, Enzyme Structure and Mechanism in Protein Science. W.H. Freeman and Company, New York, 1999.

[42] P.K. Verma, R. Saha, R.K. Mitra, S.K. Pal, Slow water dynamics at the surface of macromolecular assemblies of different morphologies, Soft Matter 6 (2010) 5971–5979.

[43] D.V. O'Conner, D. Philips, Time Correlated Single Photon Counting. Academic Press, London, 1984.

[44] B.B. Owen, H.L. Simons, Standard partial molal compressibilities by ultrasonics. I. Sodium chloride and potassium chloride at 25°, J. Phys. Chem. 61 (1957) 479–482.

[45] S. Barnartt, The velocity of sound in electrolytic solutions, J. Chem. Phys. 20 (1952) 278–279.

[46] R.P. Rand, N.L. Fuller, P. Butko, G. Francis, P. Nicholls, Measured change in protein solvation with substrate-binding and turnover, Biochemistry 32 (1993) 5925–5929.

[47] J.P. Hennessey, W.C. Johnson, Information content in the circular dichroism of proteins, Biochemistry 20 (1981) 1085–1094.

[48] B.J. Jordan, R. Hong, B. Gider, J. Hill, T. Emrick, V.M. Rotello, Stabilization of α-chymotrypsin at air–water interface through surface binding to gold nanoparticle scaffolds, Soft Matter 2 (2006) 558–560.

[49] J.A. Rodríguez-Martínez, R.J. Solá, B. Castillo, H.R. Cintrón-Colón, I. Rivera-Rivera, G. Barletta, K. Griebenow, Stabilization of α-chymotrypsin upon PEGylation correlates with reduced structural dynamics, Biotechnol. Bioeng. 101 (2008) 1142–1149.

[50] I.J. Castellanos, W. Al-Azzam, K. Griebenow, Effect of the covalent modification with poly(ethylene glycol) on α-chymotrypsin stability upon encapsulation in poly(lactic-co-glycolic) microspheres, J. Pharm. Sci. 94 (2005) 327–340.

[51] A.R. Fersht, Catalysis, binding and enzyme-substrate complementarity, Proc. R. Soc. Lond. B 187 (1974) 397–407.

[52] J.R. Giorgione, R.M. Epand, Role of water in protein kinase C catalysis and its binding to membranes, Biochemistry 36 (1997) 2250–2256.

[53] J. Rodríguez-Martínez, I. Rivera-Rivera, R. Solá, K. Griebenow, Enzymatic activity and thermal stability of PEG-α-chymotrypsin conjugates, Biotechnol. Lett. 31 (2009) 883–887.

[54] A. Zaks, A.M. Klibanov, Enzymatic catalysis in nonaqueous solvents, J. Biol. Chem. 263 (1988) 3194–3201.

[55] H.C. Chiu, S. Zalipsky, P. Kopeckova, J. Kopecek, Enzymic activity of chymotrypsin and its poly(ethylene glycol) conjugates toward low and high molecular weight substrates, Bioconjugate Chem. 4 (1993) 290–295.

[56] Formulization of equation (12) is quite a controversial issue in the literature. This equation formulated by the group of Rau, Rand and Parsegian has been analytically criticised (PNAS 95 (1998) 7363; PNAS 99 (2002) 9721). The issue is related to the inclusion of the activity of PEG in the total free energy expression. According to Parsegian, et al. (PNAS 97 (2000) 3987) this exclusion is taken care by the Gibbs–Duhem equation which connects the two activity terms in the bulk. For any conformational change in the protein hydration state upon addition of PEG, a linear relationship between the osmotic stress and the free energy change in the protein could be drawn including a constant term ΔN_{ew}^{ab}, which denotes the excess (or deficite) number of water molecules at the protein hydration layer upon a conformational transition of state 'a' to 'b'. This linearity however breaks at high PEG concentration owing to preferential inclusion of PEG at the protein surface.

[57] V.A. Parsegian, R.P. Rand, D.C. Rau, Osmotic stress, crowding, preferential hydration, and binding: a comparison of perspectives, Proc. Natl. Acad. Sci. U.S.A. 97 (2000) 3987–3992.

[58] M.F. Colombo, G.O. Bonilla-Rodriguez, The water effect on allosteric regulation of hemoglobin probed in water/glucose and water/glycine solutions, J. Biol. Chem. 271 (1996) 4895–4899.

[59] M. Colombo, D. Rau, V. Parsegian, Protein solvation in allosteric regulation: a water effect on hemoglobin, Science 256 (1992) 655–659.

[60] I. Vodyanoy, S.M. Bezrukov, V.A. Parsegian, Probing alamethicin channels with water-soluble polymers. Size-modulated osmotic action, Biophys. J. 65 (1993) 2097–2105.

[61] N.Y. Sidorova, D.C. Rau, Differences in water release for the binding of EcoRI to specific and nonspecific DNA sequences, Proc. Natl. Acad. Sci. U.S.A. 93 (1996) 12272–12277.

[62] J.J.M. Bergeron, J. Paiement, R. Rachubinski, N.M.K. Ng Ying Kin, R. Sikstrom, Membrane fusion and the mechanism of terminal glycosylation within the golgi apparatus of rat liver hepatocytes, Biophys. J. 37 (1982) 121–122.

[63] P.G. Merzlyak, L.N. Yuldasheva, C.G. Rodrigues, C.M.M. Carneiro, O.V. Krasilnikov, S.M. Bezrukov, Polymeric nonelectrolytes to probe pore geometry: application to the ±-toxin transmembrane channel, Biophys. J. 77 (1999) 3023–3033.

[64] B. Gavish, E. Gratton, C.J. Hardy, Adiabatic compressibility of globular proteins, Proc. Natl. Acad. Sci. U.S.A. 80 (1983) 750–754.
[65] T.V. Chalikian, K.J. Breslauer, Compressibility as a means to detect and characterize globular protein states, Proc. Natl. Acad. Sci. U.S.A. 93 (1996) 1012–1014.
[66] A.A. Zamyatnin, Amino acid, peptide, and protein volume in solution, Ann. Rev. Biophys. Bioeng. 13 (1984) 145–165.
[67] T.V. Chalikian, M. Totrov, R. Abagyan, K.J. Breslauer, The hydration of globular proteins as derived from volume and compressibility measurements: cross correlating thermodynamic and structural data, J. Mol. Biol. 260 (1996) 588–603.
[68] T.V. Chalikian, J. Völker, D. Anafi, K.J. Breslauer, The native and the heat-induced denatured states of α-chymotrypsinogen A: thermodynamic and spectroscopic studies, J. Mol. Biol. 274 (1997) 237–252.
[69] G. Graziano, Non-intrinsic contribution to the partial molar volume of cavities in water, Chem. Phys. Lett. 429 (2006) 420–424.
[70] D.P. Kharakoz, A.P. Sarvazyan, Hydrational and intrinsic compressibilities of globular proteins, Biopolymers 33 (1993) 11–26.
[71] T.V. Chalikian, A.P. Sarvazyan, K.J. Breslauer, Hydration and partial compressibility of biological compounds, Biophys. Chem. 51 (1994) 89–109.
[72] J.D. Johnson, M.A. El-Bayoumi, L.D. Weber, A. Tulinsky, Interaction of α-chymotrypsin with the fluorescent probe 1-anilinonaphthalene-8-sulfonate in solution, Biochemistry 18 (1979) 1292–1296.
[73] E.L. Mertz, L.I. Krishtalik, Low dielectric response in enzyme active site, Proc. Natl. Acad. Sci. U.S.A. 97 (2000) 2081–2086.
[74] D.C. Turner, L. Brand, Quantitative estimation of protein binding site polarity. Fluorescence of N-arylaminonaphthalenesulfonates, Biochemistry 7 (1968) 3381–3390.
[75] R. Jimenez, G.R. Fleming, P.V. Kumar, M. Maroncelli, Femtosecond solvation dynamics of water, Nature 369 (1994) 471–473.
[76] W. Jarzeba, G.C. Walker, A.E. Johnson, M.A. Kahlow, P.F. Barbara, Femtosecond microscopic solvation dynamics of aqueous solutions, J. Phys. Chem. 92 (1988) 7039–7041.
[77] N. Nandi, K. Bhattacharyya, B. Bagchi, Dielectric relaxation and solvation dynamics of water in complex chemical and biological systems, Chem. Rev. 100 (2000) 2013–2045.
[78] B. Bagchi, Water dynamics in the hydration layer around proteins and micelles, Chem. Rev. 105 (2005) 3197–3219.
[79] N. Nandi, B. Bagchi, Dielectric relaxation of biological water, J. Phys. Chem. B 101 (1997) 10954–10961.
[80] S.K. Pal, J. Peon, B. Bagchi, A.H. Zewail, Biological water: femtosecond dynamics of macromolecular hydration, J. Phys. Chem. B 106 (2002) 12376–12395.
[81] K. Sahu, S.K. Mondal, S. Ghosh, D. Roy, P. Sen, K. Bhattacharya, Temperature dependence of solvation dynamics and anisotropy decay in a protein. ANS in bovine serum albumin, J. Chem. Phys. 124 (2006) 124907–124909.
[82] S.K. Pal, J. Peon, A.H. Zewail, Ultrafast surface hydration dynamics and expression of protein functionality: α-chymotrypsin, Proc. Natl. Acad. Sci. U.S.A. 99 (2002) 15297–15302.